Interreg
EUROPEAN UNION
North-West Europe
Care-Peat
European Regional Development Fund

# Interreg Care-Peat

## Deliverable T1 3.2
## Development, calibration and validation of a numerical model for C-fluxes

**Nicolas DEVAU, Sébastien GOGO and Laurent ANDRE**

| Name | Organisation |
|---|---|
| Nicolas DEVAU | BRGM – French Geological Survey |
| Sébastien GOGO | University of Rennes 1 |
| Laurent ANDRE | BRGM – French Geological Survey |

# Revision history

| Date | Author | Description |
|---|---|---|
| 30/06/2021 | N. Devau, S. Gogo, L. André | Draft version |
| 06/09/2021 | P. Audigane (BRGM) | Review |
| 22/09/2021 | A. Saada (BRGM) | Approbation |

# General information

| | |
|---|---|
| **Deliverable** | Deliverable T1 3.2 |
| **Deliverable name** | Development, calibration and validation of a numerical model for C-fluxes |
| **Deadline deliverable** | 30 June 2021 |
| **Status** | Final report |
| **Remarks, Summary of activities** | This report presents the main developments made about the numerical model developed to estimate C-fluxes from peatlands. It is based on a number of relevant parameters describing the hydrological and hydrogeological functioning of the peatland area including the weather conditions like the temperature or the recharge. This model allows calculating the variations of soil water content but also the C emissions due to respiration processes. It is fitted on long-term measurements performed on La Guette peatland (FR). |

Public document

# Development, calibration and validation of a numerical model for C-fluxes

Final Report

**BRGM/RP-71118-FR**
June 2021

Study carried out as part of
activities in the INTERREG NWE CARE-PEAT Project

**N. Devau, S. Gogo, L. André**
With the collaboration of all the partners of the CARE-PEAT Project

| **Checked by:** | **Approved by**: |
|---|---|
| Name: P. Audigane | Name: A. Saada |
| Function : Hydrogeologist | Regional Director Centre Val de Loire |
| Date: 06/09/2021 | Date: 22/09/2021 |
| Signature: | Signature: |

**The quality management system of BRGM is certified according to ISO 9001 and ISO 14001.**

**Contact : qualite@brgm.fr**

Interreg North-West Europe Care-Peat
European Regional Development Fund

Geoscience for a sustainable Earth
brgm

**Keywords**: peatlands, greenhouse gases, geochemical modelling

In bibliography, this report should be cited as follows:

Devau N., Gogo S., André L. (2021) - Development, calibration and validation of a numerical model for C-fluxes. Report BRGM/RP-71118-FR, 25 p.

# Synopsis

Many recent studies underline the strong feedbacks between hydrological changes in peatland and $CO_2$ fluxes associated with ecosystem respiration (ER) and growth primary production (GPP).

To improve understanding of the interaction between hydrology and greenhouse gas emissions, several numerical tools have been developed during the last decades to simulate $CO_2$ emissions according to changes in hydrology, especially to assess if peatland will act as a C-source or-sink term in response to climate change. However, the model diversity seems to illustrate that there is currently no single model suitable for application to peatland in either temperate, boreal or tropical conditions.

In this context, the main objective of the work presented in this report was to assess the efficiency of reactive transport model to investigate feedbacks between hydrological changes in peatland and $CO_2$ fluxes associated with ER in a peatland. For this purpose, a variably saturated flow model and a reactive transport model were build using the HPx software (Jacques et al., 2018) to simulate water content at different depths as well as $CO_2$ fluxes issued from aerobic respiration at the soil-atmosphere interface.

The results of this work demonstrated that reactive transport model was suitable to investigate feedbacks between hydrological changes and $CO_2$ fluxes associated with ER in a peatland. This model take into account the complex interactions between soil hydrology, thermal dynamics and aerobic respiration reaction. It is applied with success to the La Guette peatland site (FR).

# Table of contents

# Table of figures

# Introduction

Temperate peatlands are important component of the global carbon cycle due to large carbon pools resulting from the long-term accumulation of organic matter in peat soils (Turunene et al., 2002). Ecosystem respiration (ER) and growth primary production (GPP) are vulnerable to changes in hydrology. However, the response of these two processes to hydrological change can be unclear. Lowering of the water tables exposes peat soils to oxygen resulting in higher rate of aerobic respiration reaction supporting ER and promoting $CO_2$ diffusion by gas phase connectivity. This effects has been observed in both laboratory and field studies (Silvola et al., 1996; Sulman et al., 2009). Recently, Evans et al. (2021) found that the mean annual effective water table depth had a large impact on greenhouse gas fluxes. A reduction of 10 centimeters in mean water table depth implies a decrease by the equivalent of at least 3 tons of $CO_2$ by hectare per year, until water table depth is less than 30 centimeters. These results have been obtained by analyzing water balance and greenhouse gas fluxes from 41 peatlands located in the UK and Ireland. Nevertheless, some studies have pointed out that very dry conditions can be associated with lower rates of ER as low soil water content can inhibit or decrease rate of aerobic respiration driven by microbial biomass (Parton et al., 1987). This trend has been also reported by Parmentier et al. (2009) in a peatland in Netherlands. These results underline the strong feedbacks between hydrological changes in peatland and $CO_2$ fluxes associated with ER and GPP.

To improve understanding of this interaction between hydrology and greenhouse gas emissions, several numerical tools have been developed to simulate $CO_2$ emissions according to changes in hydrology, especially to assess if peatland will act as a C-source or-sink term in response to climate change. First, analytical model have been developed to simulate this feedback between carbon cycle and water table depth. Nevertheless, fast-timescale processes, especially changes in rate of aerobic respiration have not been incorporated due to mathematical limitations (Ise et al., 2008). This analytical model are often integrated in ecosystem model, which has been usually used to simulate evolution of carbon cycle under climate change at peatland scale. Sulman et al. (2012) have performed model benchmark to assess efficiency of ecosystem models to reproduce $CO_2$ fluxes at three wetland sites in Canada and the northern United States. Models consistently overestimated mean annual growth ecosystem production and ecosystem respiration. Models that taken into account a more refine description of water table dynamic had less bias than models that did not. These authors recommended updating ecosystem models by including a physical-based description of the interactions between hydrology and carbon cycle. Aware of the limit of ecosystem model, several works have been devoted to build a more physical-based model to simulate greenhouse gas fluxes issued from peatland. During the last decades, literature data seems to indicate that dozens of model have been developed or adapted to perform such simulations. For instance, Farmer et al. (2011) have reviewed the main characteristics of some of the physical-based models (SIMGRO, MWM, Yasso, MERES, LPJ, ECOSSE, PEATLAND, PnET-N-DNDC) elaborated to simulate greenhouse gas emissions from peatlands. This model diversity seems to illustrate that there is currently no single model suitable for application to peatland in either temperate, boreal or tropical conditions. Development of

an integrated physical-based simulation model of peatland biogeochemistry seems difficult because of the challenges of simulating simultaneously physical aspects such as soil hydrology, thermal dynamics and biogeochemical thermodynamically and kinetically-controlled reactions as well as the lack of computational and conceptual modelling frameworks. As pointed out by Steefel et al. (2005), reactive transport models are robust and interpretative tool to unravel complex interactions between coupled processes and the effects of multiple space and time scales in Earth sub-surface systems. From this point of view, reactive transport simulation provides means to evaluate the relative importance and role of fundamental processes in complex environment and these tools could be obviously used in forecasting. Reactive transport models have therefore a key role in scientific investigation of complex natural systems where individual time and space-dependent processes are linked and where the relative importance of individual or sub-processes cannot be fully assessed without considering them in the context of the other dynamic processes at work.

In this context, the main objective of this work was to assess the efficiency of reactive transport model to investigate feedbacks between hydrological changes in peatland and $CO_2$ fluxes associated with ER in a peatland. For this purpose, a variably saturated flow model and a reactive transport model were build using the HPx software (Jacques et al., 2018) to simulate water content at different depths as well as $CO_2$ fluxes issued from aerobic respiration at the soil-atmosphere interface. First, the conceptual and mathematical models developed to simulate experimental data will be detailed. Then site description of the La Guette Peatland (FR), monitoring scheme used to measure $CO_2$ fluxes as well as the initial and boundary conditions taken into account will be described. The model goodness-of-fit will be showed. By interpreting results provided by simulations, hypothesis on the main processes driven $CO_2$ emissions from the La Guette peatland will be given.

# Chapter 1: Materials and Methods

## 1.1 CONCEPTUAL MODEL

In the present model developed in the study, soil profile in peatland is assumed to be a porous media, which has been modelled by accounting for a continuum representation. This approach is based on averaging system properties over a macroscopic length, called representative elementary volume (REV, see Figure 1), containing the three main phases that could be encountered in such systems: water ($\theta_w$), air ($\theta_a$) and solid phases ($\varepsilon_s$). The water, solid and gas phases are assumed well-mixed and therefore without concentration gradients inside a REV, thus resulting in uniform reaction rates within the control volume. Flow velocity in water or gas phases is proportional to the pressure gradient. Water flow is assumed to be not impacted by gas flow. Flow and transport processes as well as biogeochemical reactions are assumed to be uniformly distributed in the control volume. The mathematical formulations used to simulate them are described below.

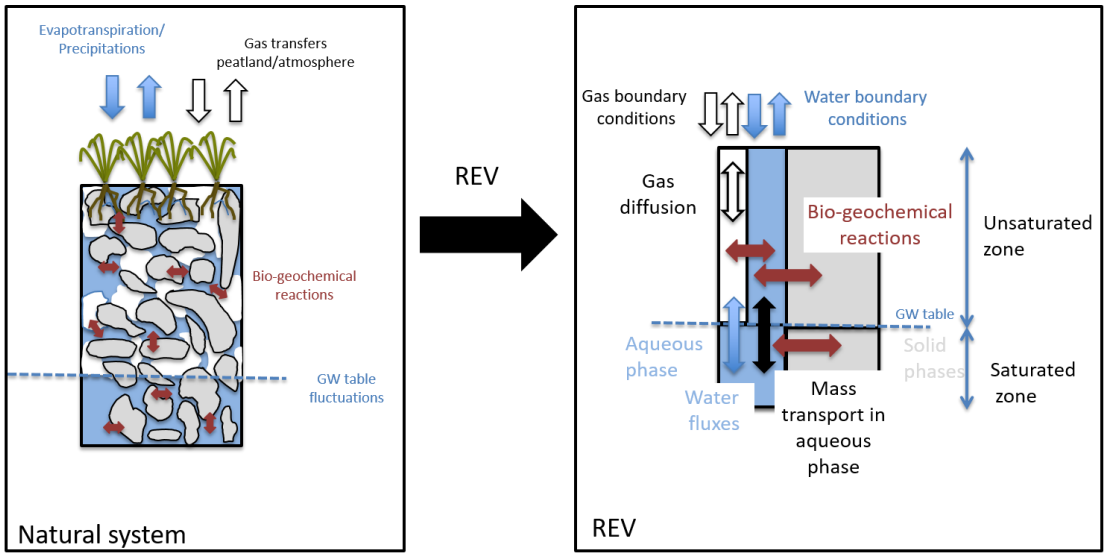


*Figure 1: Sketch illustrating the continuum representation used in macroscopic reactive transport model.*

## 1.2 MATHEMATICAL MODELS

Water flow in tis most general form is described using the Richards equation (Simunek and van Genuchten, 2008):

$$\frac{\partial \theta_w}{\partial t} = \frac{\partial}{\partial x_i}\left[K\left(K_{ij}^A \frac{\partial h}{\partial x_i} + K_{iz}^A\right)\right] - S_{r,w}$$

where $h$ is the pressure head [cm], $x$ ($i$ =1,2,3) are the spatial coordinated [cm], $t$ is time [d], $K_{ij}^A$ are components of a dimensionless anisotropy tensor $\boldsymbol{K^A}$, and K is the unsaturated hydraulic conductivity functions [m $d^{-1}$].

Several analytic forms are available to describe the unsaturated soil hydraulic properties $\theta(h)$ and $K(h)$ including Brooks and Corey (1964), van Genuchten (1980), Kosugi (1996), and Durner (1994). The Mualen and van Genuchten formalisms have been used in the present work. The pore-size distribution model of Mualem (1976) was used to predict unsaturated hydraulic conductivity function, $K(h)$, from the saturated hydraulic conductivity and van Genuchten's model (1980) of the soil water retention curve:

$$K(h) = K_s S_e^l \left[1 - \left(1 - S_e^{1/m}\right)^m\right]^2$$

where $K_s$ is the saturated hydraulic conductivity (cm $d^{-1}$), $S_e$ is the effective saturation (unitless), and $l$ and $m$ are empirical parameters (unitless). The parameter m was determined by using van Genuchten model (van Geuchten, 1980):

$$\theta_l(h) = \begin{cases} \theta_r + \dfrac{\theta_s - \theta_r}{[1 + |\alpha h|^n]^m} & h < 0 \\ \theta_s & h > 0 \end{cases}$$

where $\theta_s$ and $\theta_r$ are the saturated and residual water contents ($dm^3\ dm^{-3}$), respectively, and $\alpha$ ($m^{-1}$), n (unitless) and $m\,(= 1 - 1/n)$ are empirical shape parameters. In the present model, boundary conditions are assumed system-dependent by considering atmospheric conditions involving time-dependent precipitation, potential evaporation and potential transpiration rates (see below).

Heat transport is described as:

$$C_s(\theta)\frac{\partial T}{\partial t} = \frac{\partial}{\partial x_i}\left(\lambda_{ij}(\theta)\frac{\partial T}{\partial x_i}\right) - C_w q_i \frac{\partial T}{\partial x_i}$$

where $C_s$ and $C_w$ are volumetric heat capacities (J $m^{-3}$ $K^{-1}$) of soil and water, respectively, and $\lambda_{ij}$ is the apparent thermal conductivity of the soil (J $m^{-3}$ $K^{-1}$). The reactive module uses temperature to correct change rate coefficients according to the mathematical formula used in the present project (see below).

Solute concentrations in the aqueous phase are expressed in terms of total concentrations for a given primary species, $C_k$ (mol $kgw^{-1}$), which includes the concentration of all aqueous equilibrium species, $c_l$ (mol $kgw^{-1}$) or so-called secondary species:

$$C_k = c_k + \sum_{l=1}^{N_a} v_{lk} c_l$$

where $v_{lk}$ is the stoichiometric coefficient of species $k$ in secondary species $l, k = 1, \ldots N_c$ ($N_c$ is the number of primary species) and $l = 1, \ldots N_a$ ($N_a$ is the number of secondary species). For each primary species, solute transport in the aqueous phase is described using advection-dispersion-reaction equation of the form:

$$\frac{\partial \theta C_k}{\partial t} = \frac{\partial}{\partial x_i}\left(\theta D_{ij}^w \frac{\partial C_k}{\partial x_i}\right) - \frac{\partial q_i C_k}{\partial x_i} - \Gamma_{wa,k} - R_k^{eq} - R_k^{kin}$$

where $C_k$ is the total concentration of the $k$ species in the aqueous phase (mol dm$^{-3}$), respectively, $\theta$ have the unit (dm dm$^{-3}$), $D_{ij}^w$ is the dispersion coefficient tensor (m$^2$ s$^{-1}$), $q_i$ is the *i*th component of the Darcian fluid flux density (m s$^{-1}$), $\Gamma_{wa,k}$ accounts for the exchange between the aqueous and the gas phase (mol dm$^{-3}$ s$^{-1}$), $R_k^{eq}$ and $R_k^{kin}$ are aqueous sink/source terms (mol dm$^{-3}$ s$^{-1}$) with the superscripts $eq$ and $kin$ referring to equilibrium and kinetic reactions, respectively.

Diffusion in the gas phase is described as:

$$\frac{\partial \theta_a C_{a,k}}{\partial t} = \frac{\partial}{\partial x_i}\left(\theta_a D_{ij}^a \frac{\partial C_{a,k}}{\partial x_i}\right) + \Gamma_{wa,k}$$

where $C_{a,k}$ is the concentration in the gas phase of component $k$ (mol dm$^{-3}$), $D_{ij}^a$ is the gaseous diffusion tensor (m$^2$ s$^{-1}$).

The geochemical model calculates aqueous concentrations of the primary and secondary species using an aqueous equilibrium chemical model written as:

$$A_l \rightleftharpoons \sum_{k=1}^{N_c} \upsilon_{lk} A_k$$

where $A_l$ and $A_k$ are the chemical formulae of the species, $\upsilon_{lk}$ are stoichiometric coefficients and $N_c$ is the number of primary species. Mass action laws permit calculations of the aqueous concentrations as follows:

$$C_l = \frac{\prod_{k=1}^{N_c} (\gamma_k c_k)^{\upsilon_{lk}}}{K_l \gamma_l}$$

where $K_l$ is the equilibrium constant for the reaction, defined as product of the activities of the reaction products divided by the product of the activities of the reactants, and $\gamma_k$ and $\gamma_l$ are the activity correction to obtain activity $\alpha$ (unitless) when multiplied with $c$. The thermodynamic contants are adapted for temperature using the enthalpy of the reaction in the van't Hoff equation or by a six-term analytic equation as a function of temperature (Parkhurst and Appelo, 2013). Several activity correction models could be selected. The extended Debye-Huckel equation has been used.

The ecosystem respiration is assumed to be mainly driven by heterotrophic aerobic respiration driven by microbial biomass. This reaction could be written in a generic form as follow:

$$SOM + O_2 \rightleftharpoons CO_2 + H_2O$$

Literature data indicates that this reaction is mainly kinetically constrained, allowing us to use mathematical formalism which do not account for thermodynamic parameter. Hence, a linear mass balance equation was used to describe aerobic respiration driven by microbial activity. This equation assumes that both substrate and microbial biomass are not limiting factors:

$$\frac{\partial C_{CO2}}{\partial t} = k \quad C_{SOM}$$

where $C_{CO2}$ is the $CO_2$ concentration issued from aerobic respiration (mol kgw$^{-1}$), $k$ is the first-order decomposition term (s$^{-1}$), $C_{SOM}$ is the concentration of soluble organic matter (mol kgw$^{-1}$). The value of $k$ depend on soil temperature, $f_T(T)f_m$, and soil moisture, $f_m(S_\theta)$, as follows:

$$k = k_0 f_T(T) f_m(S_\theta)$$

where $k_0$ is the reference rate (s$^{-1}$). Several works gave an overview of different functions to account for the effects of several environmental factors (Sierra et al., 2012). The function proposed par Porporato et al. (2003)

$$f_m(S_\theta) = \begin{cases} 1 - \dfrac{\theta - \theta_r}{\theta_s - \theta_r} & \theta \leq \theta_s \\ 1 & \theta \geq \theta_s \end{cases}$$

The temperature dependency is described using the formulation from ROTC (Jenkinson et al., 1990):

$$f_T(T) = \frac{47.9}{1 + \exp(\frac{106}{T + 18.3})}$$

## 1.3 BOUNDARY CONDITIONS

For flow, the top boundary of the column is defined as prescribed fluxes based on daily potential water fluxes, calculated as the difference between rainfall and potential evaporation. A transient boundary condition is applied at the bottom according to water table level measurements recorded. The modified Penmn-Monteith equation was used to calculate potential evapotranspiration:

$$ET_0 = ET_r + ET_a = \frac{1}{\lambda}\left[\frac{\Delta(R_n - G)}{\Delta + \gamma[1 + (r_c/r_a)]}\right] + \frac{\rho_a c_p (e_a - e_d)/r_a}{\Delta + \gamma[1 + (r_c/r_a)]}$$

where $ET_0$ is the potential evapotranspiration rate expressed by a soil water layer thickness evaporated by day (mm d$^{-1}$), $ET_r$ is the radiation term (mm d$^{-1}$), $ET_a$ is the aerodynamic term (mm d$^{-1}$), $\Delta$ is the slope of the saturation vapor pressure curve as a function of temperature ($e_a = f(T)$) (kPa °C$^{-1}$), $R_n$ is net radiation (MJ m$^{-2}$ d$^{-1}$), $G$ is the soil heat flux (MJ m$^{-2}$ d$^{-1}$), $\rho_a$ is the air density (kg m$^{-3}$), $c_p$ is the specific heat of moist air (kJ kg$^{-1}$ °C$^{-1}$) ($c_p$= 1.013 kJ kg$^{-1}$ °C$^{-1}$), $(e_a - e_d)$ is the vapor pressure deficit (kPa), $e_a$ is

the saturation water vapor pressure (kPa), $e_d$ is the actual water vapor pressure (kPa), $r_a$ is the aerodynamic resistance (s $m^{-1}$), $\lambda$ is the latent heat of vaporization (MJ $kg^{-1}$), $\gamma$ is the psychometric constant (kPa $°C^{-1}$) and $r_c$ is the canopy resistance (s $m^{-1}$).

Aerodynamic resistance of reference grass canopy is expressed in the FAO procedure (Allen et al., 1998) as follows:

$$r_a = \frac{ln\left[\frac{z_m - d_e}{z_{om}}\right] ln\left[\frac{z_h - d_e}{z_{oh}}\right]}{\kappa^2 u_z} = \frac{208}{u_z}$$

where $z_m$ and $z_h$ are heights of the wind speed and of the temperature and the humidity measurements (m), $d_e$ is the zero plane displacement height (m), $z_{oh}$ is the roughness length governing transport of the heat and the vapor (m), $u_z$ is the wind speed at the height 2 m and $\kappa$ is the von Karman constant (unitless).

Crop canopy resistance is:

$$r_a = \frac{r_l}{0.5LAI} = \frac{200}{LAI}$$

where $r_l$ is the daily average bulk stomata resistance of the well illuminated leaf (s $m^{-1}$) and LAI is the active leaf area index.

A Cauchy-type boundary condition is applied at the top boundary for gas fluxes. $CO_2$ influx or outflux are allowed depending on the difference of partial pressure between atmosphere and the gaseous phase in the unsaturated cells. If $CO_2$ partial pressure is higher in the soil gaseous phase than atmosphere, $CO_2$ outflux occurs. If opposite conditions are encountered, $CO_2$ influx is simulated. No gas fluxes occurs when cell water content is equal to saturated water content. A closed boundary condition is assumed at the bottom of the column.

For solute transport, Cauchy-type boundary conditions are also used at the top boundary. During rainfall events, the top boundary is defined as prescribed flux for solute transport, while under evaporative conditions, the top boundary changes and is closed for solute transport, leading to solute being retained and causing concentration build-up. At the bottom, a fixed concentration is set. For temperature, transient boundary conditions was used at the top and bottom of the column.

## 1.4 SOFTWARE

The model was build using the HPx code coupling the HYDRUS-1D software (Simunek et al., 2016) with PHREEQC software (Parkhurst and Appelo, 2013). It solves the coupled reactive-transport equations using sequential non-iterative approach (Figure 2). HYDRUS-1D act as the solver for the hydrological and physical processes, including variable-saturated water flow, solute transport, diffusion in the gas phase and heat transport, whereas PHREEQC is the solver for the thermodynamic and kinetic (bio)-geochemical reactions.

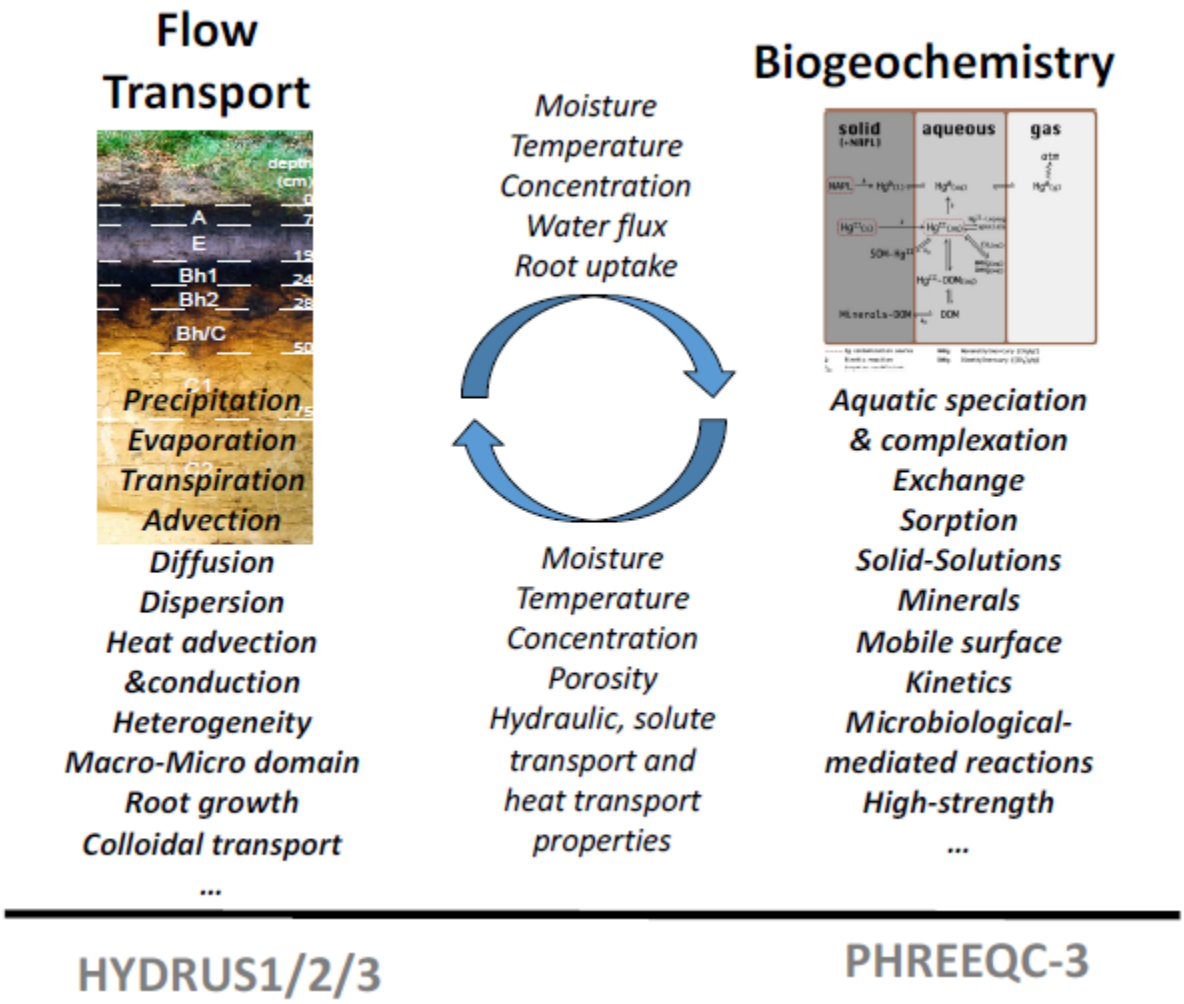


*Figure 2 : Main capabilities and reactive transport processes simulated by the code HPx (Jacques et al., 2018)*

# Chapter 2: Application and discussion

## 2.1 SITE DESCRIPTION

The numerical model developed in the present work has been developed to simulate water and $CO_2$ fluxes measured in La Guette peatland. This site is a Sphagnum peatland located in France (Neuvy-sur-Barangeon, Cher, N 47°1944, E 2°1704). It is a transitional poor fen (with a pH between 4 and 5 and a conductivity lower than 80 µS $m^{-2}$) with a maximum peat thickness of about 180 cm. Mean annual temperature was 11°C and mean annual rainfall 732 mm for the period 1971-2000 (Gogo et al., 2011). The site is drained in its south part by a road built before 1945 that crosses the peatland. In 2009, the drainage ditch of the road was scraped, lowering the output level and consequently increasing the water losses. This hydrological disturbance has probably contributed to the invasion of the site by vascular plants, mainly *Pinus sylvestris*, *Betula spp.* (*Betula verrucosa* and *pubescens*) and *Molinia caerulea*. This *Poaceae* is now invading numerous peatlands in Europe mainly, due to an increase of the nitrogen deposition and drainage (D'Angelo et al., 2021) and thus at the detriment of the specific peatland species composed of *Sphagnum cuspidatum* and *Sphagnum rubellum*, *Eriophorum augustifolium*, *Erica tetralix* and *Calluna vulgaris*.

## 2.2 MONITORING OF ENVIRONMENTAL PARAMETERS AND $CO_2$ FLUXES

Several meteorological variables, including total rainfall, net solar radiation, atmospheric pressure, wind direction and speed, air temperature and humidity were automatically monitored at a daily frequency during the entire studied period by using two automatic stations installed on the site since November 2010. A similar device was used to monitor soil water content and soil temperature at -2, -5, -10, -20 and -40 cm depths. Measurements have been recorded since September 2017 to November 2020. During the same period, water table level was also recorded below the position of the meteorological stations as well as on two other locations (Binet et al., 2013). Greenhouse gas emissions have been investigated using an eddy-covariance station that was installed in early September 2017. Fluxes were measured every 15 minutes and were used to calculate net ecosystem exchange (NEE). Fluxes measured at night conditions were used to estimate ER. These two variables were used to estimate Growth Primary Production (GPP). Raw data have been cleaned and filtered before to be used (Jacotot et al, in prep.). For instance, missing values in the time series have been estimated by interpolating data. Furthermore, data have been filtered to remove outliers and abnormal data.

## 2.3 INITIAL CONDITIONS

Water and gas flow as well as solute transport have been simulated in a one-dimensional partially saturated column with a depth of 100 cm, mimicking a soil profile. This column has been divided in 100 cells of 1cm length. Two sub-domains have been considered in

the model. The first was ranging from the surface to 5 cm depth while the second is located below. Physical properties for the flow and transport models as well as the rate of the aerobic respiration reaction used in the two sub-domains are listed in Table 1.

| | $\theta_r$ | $\theta_s$ | $\alpha$ ($cm^{-1}$) | n | l | $K_s$ ($cm.d^{-1}$) | $D_L$ (cm) | $D_g$ ($cm^2\ d^{-1}$) |
|---|---|---|---|---|---|---|---|---|
| Zone 1 | 0.15 | 0.5 | 0.036 | 1.56 | 0.5 | 29.5 | 1 | 1240 |
| Zone 2 | 0.5 | 0.8 | 0.036 | 1.56 | 0.5 | 29.5 | 1 | 1240 |

*Table 1: Values of flow and transport parameter as well as aerobic respiration rate used in the two sub-domains along soil profile (Zone 1: 0-5 cm depth and Zone 2: 5-100 cm depth). Values of the parameters have been calibrated to reproduce measured data (see below)*

Values of the model parameters used to simulate heat transport are given in Table 2. Default values have been used in absence of information. We assumed that the parameter values were identic in the two sub-domains.

| | $b_1$ ($W\ m^{-1}\ K^{-1}$) | $b_2$ ($W\ m^{-1}\ K^{-1}$) | $b_3$ ($W\ m^{-1}\ K^{-1}$) | $C_s$ ($J\ m^{-3}\ K^{-1}$) | $C_w$ ($J\ m^{-3}\ K^{-1}$) | $D_L$ (cm) |
|---|---|---|---|---|---|---|
| Zone 1 | $1.6 \times 10^{16}$* | $2.5 \times 10^{16}$ | $9.9 \times 10^{16}$* | $1.9 \times 10^{14}$ | $3.1 \times 10^{14}$ | 5 |
| Zone 2 | $1.6 \times 10^{16}$ | $2.5 \times 10^{16}$ | $9.9 \times 10^{16}$ | $1.9 \times 10^{14}$ | $3.1 \times 10^{14}$ | 5 |

*Table 2: Values of heat transport parameter used in the two sub-domains along soil profile (Zone 1: 0-5 cm depth and Zone 2: 5-100 cm depth).*

A pressure head of -150 cm is set. Aqueous phase is assumed to be in equilibrium with atmosphere (see Table 2). In addition, NaCl concentration is fixed at 0.01 mol $kgw^{-1}$ to fix ionic strength in order to prevent convergence problems. Recharge water is also assumed to be in equilibrium with atmosphere. An infinite concentration of Br ($1x10^{-8}$ mol $kgw^{-1}$) is also added to the recharge solution to be used as a conservative tracer. In gaseous phase, atmospheric $CO_2$ partial pressure is set at initial conditions.

## 2.4 BOUNDARY CONDITIONS

As presented in Chapter 1, the modified Penmn-Monteith equation was used to calculate potential evapotranspiration. We are aware that this equation has been developed to simulate potential evapotranspiration of “reference“ grass canopy far from the species encountered in La Guette site. Despite this gap, this modelling framework remains the most suitable to estimate temporal change in water vapor fluxes in absence of direct measurements. In addition, it implies that the model develop to La Guette site could be easily extended to other sites where standard meteorological variable are recorded, promoting the model flexibility and robustness.

The atmosphere temperature daily recorded at La Guette was used as input data as top boundary. The daily temperature at the bottom was assumed equal to the value recorded at 60 cm depth. These boundary conditions are shown in Figure 3.

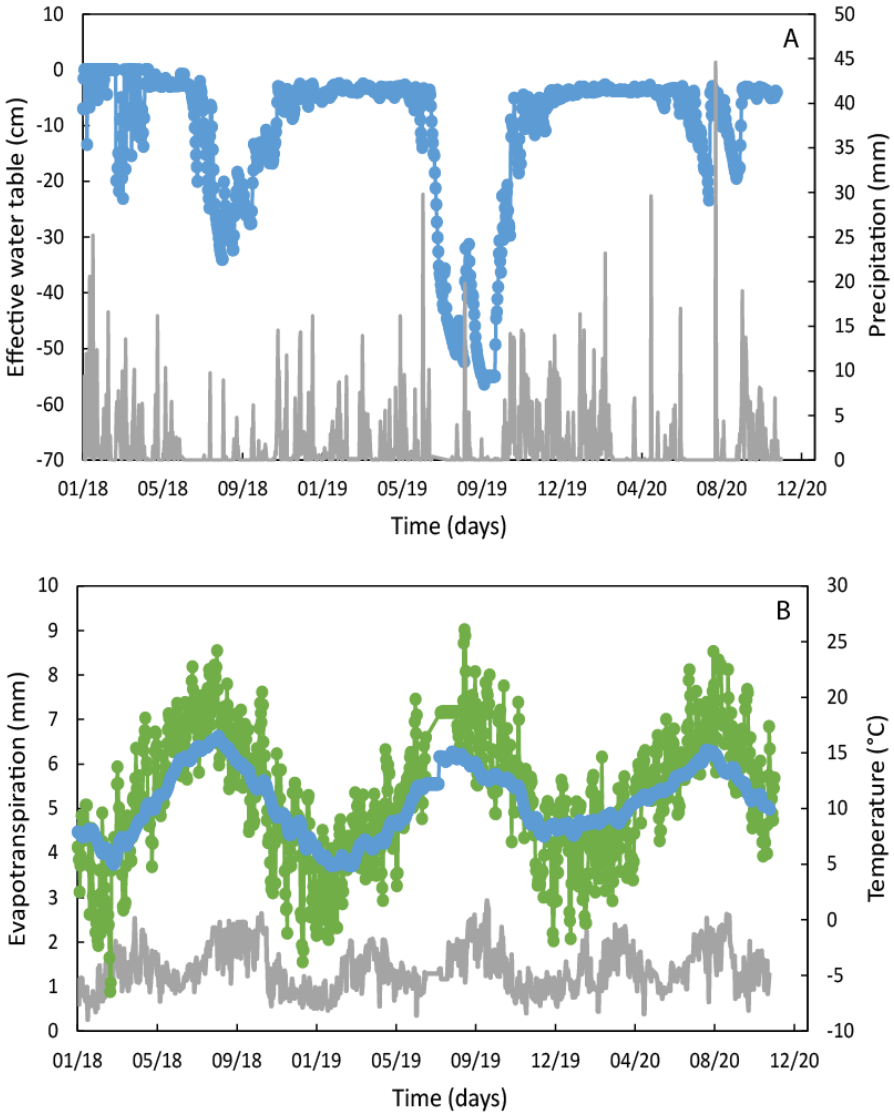


*Figure 3: Time series of A) effective water table (blue dot) and precipitations (grey line) and B) evapotranspiration (grey line), temperature at soil-atmosphere interface (green dot) and temperature at 60-cm depth (blue dot)*

## 2.5 MODEL CALIBRATION AND VALIDATION

Flow model was calibrated using soil water content measurements at -2 cm, -5 cm and -10 cm depth made from 01-01-2018 to 01-11-2020 in order to determine values for several parameters including, saturated hydraulic conductivity, the model parameters taken into account in the van Genuchten model as well as residual and saturated water content (see Table 1). Then, the reactive transport model was calibrated to simulate daily $CO_2$ fluxes associated with ER measured from 01-01-2019 to 01-11-2020. This step have enabled us to determine the value of the apparent $CO_2$ diffusion in gas phase of the porous media and the rate of $CO_2$ emissions induced by aerobic respiration reaction driven by microbial biomass (see Table 1).

To assess model goodness-of-fit, the normalized mean square error (NRMSE) was used to compare model prediction and measured values:

$$NRMSE = \frac{\sqrt{\frac{1}{n}\sum_{i=1}^{n}(p_i - m_i)^2}}{y}$$

where $n$ is the number of observations, $p_i$ the predicted values, $m_i$ the measured values and $y$ the mean value of the measured data. The closer the value of NRMSE is to 0, the better the model prediction is.

## 2.6 SIMULATIONS OF TEMPORAL CHANGES IN SOIL WATER CONTENT ACCORDING TO SOIL DEPTH

Figure 4 illustrates temporal changes in soil water content at different depths (2, 5 and 10 cm depth) in the La Guette peatland. Soil water content were lower at 2 cm depth than in deeper part of the soil profile. At 2 cm depth, water content was relatively stable during the year 2018. Soil water content ranged from 0.43 to 0.52. A decrease of soil water content was measured during the summer and autumn periods when recharge is lower than evaporation. Then, soil water content started to increase when recharge became positive again. In 2019, extreme meteorological conditions occurred in June and July with a high recharge deficit. During this period, soil water content decreased drastically from mid-June to mid-July until to reach value below probe detection limit (two weeks). Then, water content increase gradually but remained below the previous values recorded in 2018. In consequence, soil water content was lower at 2020 eve than in the same period in 2018 and 2019, approximatively half the value measured in the previous years (0.23). Soil water content progressively increased up to July. In summer period, soil water content decreased during period of recharge deficit. Soil water content reached a plate close to 0.4 in autumn period. A similar trend could be observed at 5 cm albeit the magnitude of variations was lower than that recorded in 2 cm depth. In 2018, soil water content remained stable around 0.77 during the six first months while a decrease were measured in summer and autumn periods. The lowest values measured during this period was 0.68. After this stage, soil water content increased up to reach its initial value. This value remained stable up to July 2019. Then, the soil water content decreased significantly to 0.53 (value recorded in September 2019). After this drop, a gradual increase of soil water content was monitored. The soil water content reached initial values recorded in 2018 at March 2020 and remained stable to July 2020. As recorded in the two previous years, soil water content decreased since July to October. After this period, soil water content increased in November to reach a steady value close to 0.77. At 10 cm depth, soil water content is much more stable than in upper part of the soil profile. This soil property ranged from 0.75 to 0.73. A slight decrease was measured during the summer period. In 2019, a higher decrease of soil water content was measured in summer period. The lowest value was equal to 0.64. This value was higher than the ones measured in the upper part of the soil profile during the same period. When recharge became higher than evaporation, soil water content started to increase to reach its initial value close to 0.75. No change has been measured in 2020.

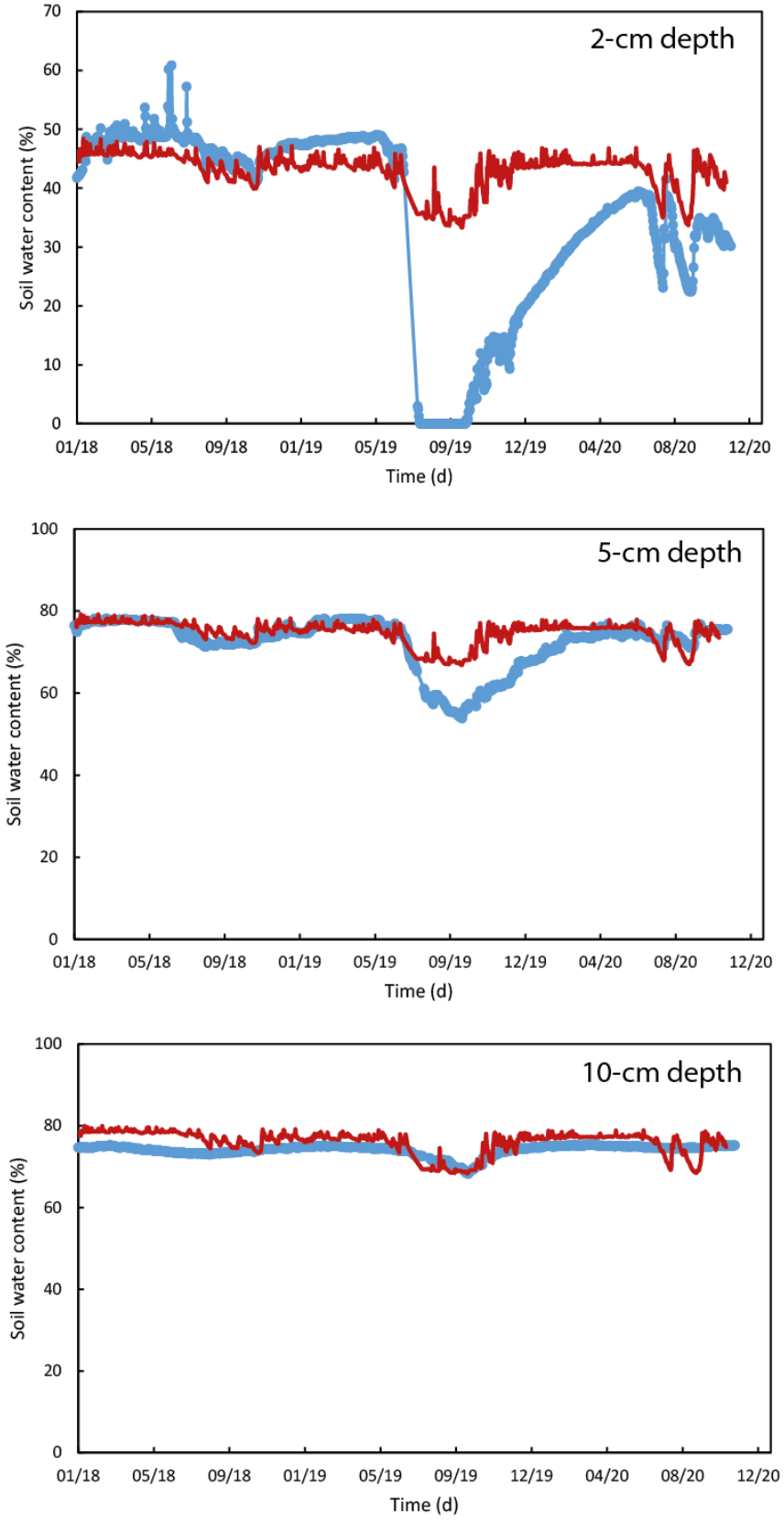


*Figure 4: Time series of soil water content at 2-cm, 5-cm and 10-cm depth, respectively. Measured values and simulations are depicted as blue dot and red line, respectively.*

Simulations results are also depicted by Figure 3. The model was able to simulate accurately soil water content from surface to 10 cm depth during year 2018 up to June 2019 (NRMSE = 0.15, 0.17, 0.19 for 2-cm, 5-cm and 10 cm depth, respectively). The decrease of soil water content during summer and autumn period is reproduced, showing that impact of recharge deficit on soil water content is correctly simulated. At 10 cm depth, simulated values are slightly higher than the measured ones. Nevertheless, the model is suitable to reproduce the main trend.

From July 2019, model failed to reproduce the drastic decrease in soil water measured at 2-cm and 5-cm depth during period of recharge deficit (NRMSE = 0.99 and 0.97 for 2-cm and 5-cm depth). The goodness-of-fit is higher at 10 cm depth (NRMSE = 0.2). From this extreme event, the model strongly overestimated values of soil water content from July 2019 to July 2020 at 2 cm depth (NRMSE = 0.83). Furthermore, the trend is not correctly reproduced. From July 2020 to November 2020, simulations were also higher that the measured values (NRMSE = 0.53). Nevertheless, the trend is captured by the simulations. At 5-cm depth, the discrepancy between simulations and measured values occurred during a shorter period, from July 2019 to January 2020 (NRMSE = 0.78). Water dynamic recorded in 2020 is correctly reproduced, including decrease of soil water content in summer and autumn periods. At 10 cm depth, soil water content remained nearly stable (NRMSE = 0.18). This trend is reproduced by the model.

The discrepancy between modelling results and measured values illustrates that soil properties in the top layer of the peatland have evolved during extreme drought conditions. The drastic decrease of soil water content measured up to 5 cm depth during summer 2019, when extreme meteorological conditions occurred, suggests that physical structure of the peatland has been damaged during this period. We hypothesize that the extreme meteorological conditions encountered in summer 2019 have altered the physical structure of the peatland (soil density and void ratio) along the first centimeter depths due to intensive drying conditions (Camporese et al., 2006). Indeed, physical properties peatlands could be affected by reversible deformations due to variations of water content. Unfortunately, we could not include this phenomenon in our present model, implying that it has to be updated to include soil shrinkage function according to soil water content in order to be able to reproduce extreme conditions but it remains suitable in standard meteorological conditions.

## 2.7 SIMULATIONS OF TEMPORAL CHANGES IN $CO_2$ FLUXES ISSUED FROM ECOSYSTEM RESPIRATION

Figure 5 illustrates $CO_2$ fluxes time series associated with net ecosystem exchange (NEE) and ecosystem respiration (ER). During the two monitored years, seasonal change in NEE flux have been recorded. Peatland captured $CO_2$ from atmosphere due to aerobic respiration supported by oxidation of organic matter when meteorological conditions were drier and warmer, i.e. summer and autumn periods. By contrast, NEE is positive, hence $CO_2$ was emitted to atmosphere in cooler and wetter conditions corresponding to winter and early springs periods. One reader can note that ER flux exhibited also a seasonal pattern, similar to the one recorded for NEE. Higher ecosystem respiration was recorded during drier and warmer period while lower fluxes are measured during cooler and wetter periods. Albeit ER was higher during summer and autumn periods, negative values of

NEE were recorded, indicating that growth primary production is the main driver of $CO_2$ exchange at soil-atmosphere interface during these two periods. During winter and springs periods, $CO_2$ emissions of La Guette peatland seem controlled by ER. Indeed, ER values are similar to NEE values. This seasonal pattern have been identified during the two monitored years. Furthermore, $CO_2$ fluxes associated with ER are one order of magnitude higher than those corresponding to NEE, suggesting that small imbalances between fluxes issued from ER and growth primary production had strongly affected net $CO_2$ emissions to atmosphere. During the period 2019-2020, peatland as emitted 0.95 kg $CO_2$ $m^{-2}$ $y^{-1}$ to atmosphere. This fraction is small compared to the cumulated fluxes associated to ER, 4 kg CO2 $m^{-2}$ $y^{-1}$. The model was able to accurately reproduce this $CO_2$ flux (Figure 5). A high goodness-of-fit is obtained (NRMSE = 0.31). The seasonal pattern is currently simulated. Modelling results highlight that ER is higher during drier and warmer period as the rate of microbially-driven aerobic respiration reaction increased during this period, especially in the first 5 cm depth. This increase of the rate of aerobic respiration reaction is promoted by the raise of temperature during summer and early autumn period albeit the decrease of soil water content partially counterbalanced this trend. Furthermore, the decrease of soil water content along depth in the peatland increase $CO_2$ diffusion rate, hence $CO_2$ fluxes towards atmosphere. The key role of change in water table level in $CO_2$ fluxes is clearly illustrated by the results recorded and simulated in August 2020. Indeed, modelling results showed that the $CO_2$ fluxes are high, in mean 10 g CO2 $m^{-2}$ $d^{-1}$, during the first seventeen days with no precipitation. This trend is abruptly broken the 18$^{th}$ August by a storm event, leading to high precipitation (44.7 mm). Following this meteorological event, soil water content in peatland increased sharply until unsaturated zone being fully saturated. In consequence, gas phase was close to nil, preventing $CO_2$ diffusion from peatland to atmosphere. Then, $CO_2$ fluxes associated with ER decrease drastically even if aerobic respiration still occurred.

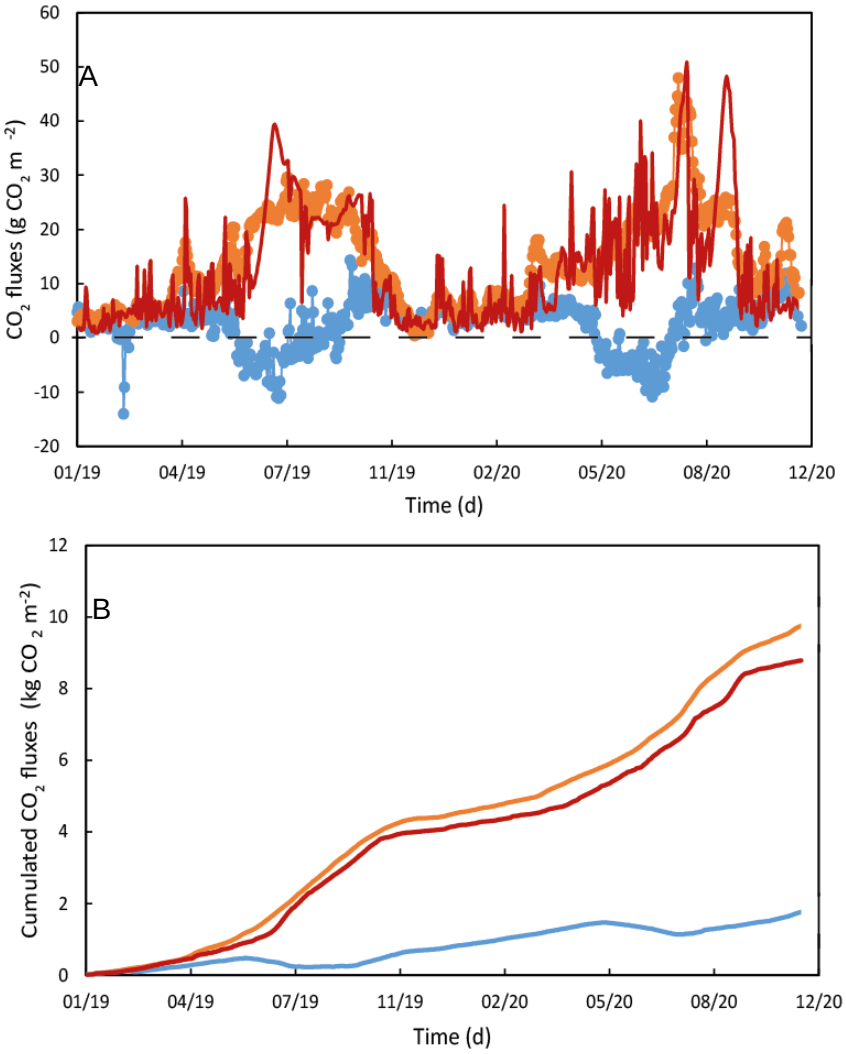


*Figure 5: Time series of A) daily $CO_2$ fluxes and B) cumulated $CO_2$ fluxes associated with ecosystem respiration (ER) and net ecosystem exchange (NEE). Measured values of ER and NEE are depicted using orange and blue dots, respectively, in the upper sub-figure and orange and blue lines, respectively, in the lower sub-figure. Red lines are used to illustrate the simulations of $CO_2$ fluxes associated with ecosystem respiration. In the upper sub-figure, dotted black line indicate that net ecosystem exchange is nil.*

# Conclusions

The present work demonstrated that reactive transport model was suitable to investigate feedbacks between hydrological changes and $CO_2$ fluxes associated with ER in a peatland. This model has taken into account the complex interactions between soil hydrology, thermal dynamics and aerobic respiration reaction. The complex changes in soil water content along soil profile recorded in La Guette was correctly reproduced during standard meteorological conditions. Model developments must be performed to simulate soil water dynamic in extreme drought conditions. Indeed, the actual model does not take into account the reversible mechanical deformation of peat in such conditions and their impact on water flows. A soil shrinkage function must be added to overcome this limit. The present results also demonstrate that a linear first order mass balance equation can be used to describe aerobic respiration at La Guette, suggesting that aerobic respiration is not limited by the amount of organic matter available for microbial respiration. Seasonal pattern in $CO_2$ fluxes associated with ecosystem respiration were correctly reproduced by the model. Modelling results demonstrated that ER is higher during drier and warmer period as the rate of microbially-driven aerobic respiration reaction increased during this period, especially in the first 5 cm depth. The higher rate of aerobic respiration reaction is induced by the raise of temperature during these periods. Nevertheless, this trend was partially counterbalanced by the decrease of soil water content. By contrast, the decrease of soil water content along depth in the peatland increase $CO_2$ diffusion rate, hence $CO_2$ fluxes towards atmosphere. These results demonstrate fast response of $CO_2$ emissions to change in soil water content not only water table level, suggesting that temporal and spatial changes in water fluxes from surface to saturated zone must be correctly assess to predict accurately $CO_2$ emissions. Last, this reactive transport model should be coupled to an ecosystem model to simulate and forecast net ecosystem exchanges.

# References


Allen R., Pereira L. S., Smith M. (1998) Crop evapotranspiration- guidelines for computing crop water requirements. FAO irrigation and drainage paper N° 56, Rome, Italy.

Brooks R. H., Corey A. (1964) Hydraulic properties of porous media. Hydrol. Paper N° 3, Colorado State Univ, Fort Collins CO.

Binet S., Gogo S., Laggoun-Défarge F. (2013) A water table dependent reservoir model to investigate the effect of drought and vascular plant invasion on peatland hydrology. *J. Hydrol.* 499, 132-139.

Camporese M; Ferraris S., Putti M., Salandin P., Teatini P. (2006) Hydrological modeling in swelling/shrinking peat soils. *Water Resour. Research* 42, 1-15.

D'Angelo B., Leroy F., Guimbaud C., Jacotot A., Zocatelli R., Gogo S., Laggoun-Défarge F. (2021) Carbon balance and spatial variability of $CO_2$ and $CH_4$ fluxes in a Sphagnum-dominated peatland in temperate climate. *Wetlands* 45, 1-20.

Durner W. (1994) Hydraulic conductivity estimation for soils with heterogeneous pore structure. *Water Resour. Research* 30(2), 211-223. DOI:10.1029/93WR02676

Evans C. D., Peacock M., Baird A. J., Artz R. R. E., Burden A., Callaghan N., Chapman P. J., Cooper H. M., Coyle M., Craig E., Cumming A., Dixon S., Gauci V., Grayson R. P., Heldter C., Heppel C. M., Holden J., Jones D. L., Kaduk J., Levy P., Matthews R., McNamara N. P., Misselbrook T., Oakley S., Page S. E., Rayment M., Ridley L. M., Stanley K. M., Williamson J. L., Worrall F., Morrison R. (2021) Overriding water table control on managed peatland greenhouse gas emissions. *Nature* 543, 548-568.

Farmer, J., Matthews R., Smith J., Smith P., Singh B. K. (2011) Assessing existing peatland models for their applicability for modelling greenhouse gas emissions from tropical peat soils. *Current Opin. Environ. Sustain.* 3, 339-349.

Ise T., Dunn A. L., Wofsi S. C., Moorcroft P. R. (2008) High sensitivity of peat decomposition to climate change through water-table feedback. *Nature geosci.* 1, 763-767.

Jacques D., Šimůnek J, Mallants D., van Genuchten M.Th. (2018) The HPx software for multicomponent reactive transport during variably-saturated flow: Recent developments and applications. *J. Hydrol. Hydromech.*, 66, 2018, 2, 211–226. DOI: 10.1515/johh-2017-0049

Jacotot A., Gogo S., Perdereau L., Paroissien J.B., Guimbaud C., Laggoun-défarge F. (in prep) High frequency measurements of $CO_2$ and $CH_4$ fluxes in a temperate peatland dominated by *Molinia caerulea* (La Guette, France).

Jenkinson D.S., (1990) The Turnover of Organic Carbon and Nitrogen in Soil. *Philosophical Transactions of the Royal Society B Biological Sciences*, 329, 361-368.

Kosugi K. (1996) Lognormal distribution model for unsaturated soil hydraulic properties. *Water Resour. Res.*, 32, 2697–2703.

Mualem Y. (1976) A new model for predicting the hydraulic conductivity of unsaturated porous media. *Water Resour. Research* 12, 513-523.

Parmentier F. J. W., van der Molen M. K., de Jeu R. A. M., Hendriks D. M. D., Dolman A. J. (2009) $CO_2$ fluxes and evaporation on a peatland in the Netherlands appear not affected by water table fluctuations. *Agricul. For. Meteor.* 149, 1201-1208.

Parkhurst D. L., Appelo C. A. J. (2013) Description of Input and Examples for PHREEQC Version 3 – A computer program for speciation, batch-reaction, one dimensional transport and inverse geochemical calculations, chapter 43 of section A. Groundwater Book 6, Modeling Techniques

Parton W., Schimel D. S., Cole C., Ojima D. (1987) Analysis of factors controlling soil organic matter levels in Great Plains grasslands. *Soil Sci. Soc. Am. J.* 51, 1173-1179.

Penman H. L. (1948) Natural evaporation from open water, bare soil, and grass. *Proc. Roy. Soc., Ser. A.* 193, 120-145.

Porprorato A., D'Odorio P., Laio F., Rodriguez Iturbe I. (203) Hydrologic controls on soil carbon and nitrogen cycles. I Modeling scheme. *Ad. Water Resour.* 26, 45-58.

Sierra C.A., Müller M., Trumbore S. E. (2012) Models of soil organic matter degradaation_ the soilR package, version 1.0 *Geosci. Model. Dev.* 5, 1045-1060.

Silvolva J., Alm J., Alholm U., Nykänen H., Martikainen P. J. (1996) CO2 fluxes from peat in boreal mires under varying temperature and moisture conditions. *Ecology* 84, 219-228.

Simunek J., van Genuchten M. T. (2008) Modeling nonequilibrium flow and transport processes using HYDRUS. *Vadose zone J.* 7, 782-797.

Simunek J., van Genuchten M. T., Sejna M. (2016) Recent developments and applications of the HYDRUS computer software packages. *Vadose Zone J.* 15, 32-45.

Steefel C. I., DePaolo D. J., Lichtner P. C. (2005) Reactive transport modeling: An essential tool and a new research approach for the Earth sciences. *Earth Planet. Sci. Lett.* 240, 539-558

Sulman B. N., Desai A. R., Cook B. D., Saliendra N., Mackay D. S. (2009) Contrasting carbon dioxide fluxes between a drying shrub wetland in Northern Winsconsin USA and nearby forests. *Biogeosciences* 6, 1115-1126.

Sulman B. N., Desai A. R., Schroede N. M., Ricciuto D., Barr A., Richardson A. D., Flanagan L. B., Lafleur P. M., Tian H., Chen G., Grant R. E., Poulter B., Verbeeck H., Ciais P., Ringeval B., Baker I. T., Schaefer K., Luo Y., Weng E. (2012) Impact of hydrological variations on modeling o peatland CO2 fluxes: Results from the North American Carbon Program site synthesis. *J. Geophys. Res.* 117, 1-21.

Turunen J., Tomppo E., Tolonen K., Reinikainen A. (2002) Estimating carbon accumulation rates of undrained mires in Finland: application to boreal and subartic regions. *Holocene* 12, 69-80

van Genuchten M. T. (1980) Closed-form equation for predicting the hydraulic conductivity of unsaturated soils. *Soil Sci. Soc. Am. J.* 44, 892-898.